Applications of SMAP Data to Retrieval of Ocean Surface Wind and Salinity

Simon Yueh*[a], Alexander Fore[a], Wenqing Tang[a], Akiko Hayashi[a], Bryan Stiles[a], Fuqing Zhang[b], Yonghui Weng[b], and Nicolas Reul[c]

[a]Jet Propulsion Laboratory, california Institute of technology, pasadena, CA 91109, USA

[b]Pennsylvania State University, University Park, PA, USA

[c]Laboratoire d'Océanographie Physique et Spatial (LOPS), Institut Français de Recherche et d'Exploitation de la MER (IFREMER), Plouzané, France

ABSTRACT

We have examined the L-band radiometer and radar data from NASA's Soil Moisture Active Passive (SMAP) mission for ocean research and applications. We find that the SMAP data are in excellent agreement with the geophysical model function (GMF) derived from the Aquarius data up to a wind speed of 20 ms^{-1}. For severe wind conditions, the higher resolution data from SMAP allowed us to assess the sensitivity of L-band radiometer signals to hurricane force winds. We applied the L-band GMF to the retrieval of ocean surface wind and SSS from the SMAP data. Comparison with the European Center for Medium-Range Weather Forecasting, WindSat and RapidSCAT wind speeds suggests that SMAP's radiometer wind speed reaches an excellent accuracy of about 1.1-1.7 ms^{-1} below a wind speed of 20 ms^{-1}. We have also found that the maximum wind speed derived from the SMAP radiometer data can reach 140 knots for severe storms and are generally in good agreement with the hurricane track analysis and operational aircraft Stepped Frequency Microwave Radiometer wind speeds. The spatial patterns of the SMAP SSS agree well with climatological distributions, but exhibit several unique spatial and temporal features.

Keywords: hurricane, microwave remote sensing, ocean surface wind, sea surface salinity, radar, radiometer

INTRODUCTION

The NASA Soil Moisture Active Passive (SMAP) Mission was recommended as the one of the tier 1 missions in the National Research Council's (NRC) Decadal Survey Report, *Earth Science and Applications from Space: National Imperatives for the Next Decade and Beyond.* The key science requirements for the SMAP mission are to provide accurate soil moisture and freeze/thaw classification for hydro-meteorology, hydro-climatology and carbon cycle studies. Soil moisture is a primary state variable of hydrology and the water cycle over land. In diverse Earth and environmental science disciplines, this state variable is either an initial condition or a boundary condition of relevant hydrologic models. Applications such as weather forecasting, and skillful modeling and forecast of climate variability and change, agricultural productivity, water resources management, drought prediction, flood area mapping, and ecosystem health monitoring all require information on the status of soil moisture. The outcomes from these applications all have direct impacts on the global environment and human society.

The NASA Soil Moisture Active Passive (SMAP) observatory was launched January 31, 2015 and started operations in April 2015. SMAP mission design uses L-band radar and radiometer for collocated, coincident measurements integrated as a single observation system [1]. The radiometer and radar share one common antenna reflector, which is a 6-m mesh deployable antenna. The antenna design consists of an offset parabola reflector with one antenna feed to produce a single antenna beam pointing at an incidence angle of about 40 degrees on the earth surface. The mesh antenna together with the feed is positioned on a spinning assembly to provide observations at two azimuth angles (fore- an aft-looks) with a conical scanning rate of about 14 rotations per minute. The resulting swath width is about 1000 km, which allows global coverage every 3 days.

@Copyrights reserved, 2016

The SMAP radiometer resolution is ~40 km, while the SMAP L-band radar provides three backscatter products: full aperture 30x30 km product, a range-sliced product at ~5 km (range) by 30 km (azimuth) resolution, and a Synthetic Aperture Radar (SAR) product at higher resolution (~1 to 3 km). The SMAP instruments have been calibrated using the data from other satellites and external targets. The calibration of the SMAP radiometer noise diode was achieved using the ocean targets and cold sky. Cross-comparison with SMOS radiometer data [2] over land and ocean surfaces indicates an excellent agreement of about 1 K.

While SMAP is primarily a land surface mission, its instrument operates at 100 percent duty cycle with data collections over ocean as well. The availability of ocean observations allows us to investigate the retrieval of sea surface wind and salinity from SMAP data. Global measurements of sea surface salinity (SSS) are important for studying the ocean circulation and water cycle and consequently for improving the estimates of seasonal to interannual climate predictions. The near surface ocean wind, generating the momentum flux affecting ocean circulation and mixing, is a key driving force in air-sea interaction processes. Measurement of near surface ocean wind vectors is crucial for many global and coastal oceanographic studies. There are also strong operational and scientific needs in monitoring the surface wind of tropical cyclones. Skillful forecasts of tropical cyclone (TC) track and intensity depend on an accurate depiction of the initial conditions of air and sea states in TC forecast models. A primary source of difficulty in past efforts for TC forecasts has been the inability to make direct observations of the surface wind field, which is one of the key driving forces for the heat and moisture exchanges between air and sea surfaces.

Many spaceborne radiometers and scatterometers with C- to Ka-band frequencies have been operating to make ocean surface wind measurements, but they are limited by reduced sensitivity to wind for hurricane force winds and the impact of rain. It is highly beneficial to develop L-band (~1 GHz) microwave wind radiometers. This is because L-band microwave sensors will be much less susceptible to rain attenuation than higher frequency sensors [3,4] and thus will fill in a critical gap for surface wind observations of severe weather systems. This has been demonstrated by the use of L-band radiometer data from ESA's Soil Moisture Ocean Salinity Mission (SMOS) for hurricane wind speed retrieval [3,4].

SMAP OCEN SURFACE WIND AND SALINITY RETREIVAL

We apply the SMAP and Aquarius Geophysical Model Functions (GMFs) to the retrieval of ocean surface wind from the SMAP radiometer data by leveraging the QuikSCAT algorithms to account for the two-look geometry (fore and aft looks from the conical scan) and dual-polarization observations. The SMAP radiometer data are binned on rectangular grids at 25 km spacing with their axes aligned with the along and across track directions of satellite [5]. To account for the directional dependence we average the data separately for the data collected from fore and aft looks, therefore reducing the data into two looks.

We use the following quadratic cost function for retrieving the hurricane wind speed (w) and direction (ϕ) from T_{BV} and T_{BH}:

$$C_{HW}(w,\phi) = \sum_{i=1}^{2} \frac{(T_{BVi} - T_{BVMi})^2}{\Delta T_{BV}^2} + \sum_{i=1}^{2} \frac{(T_{BHi} - T_{BHMi})^2}{\Delta T_{BH}^2} \quad (1)$$

The T_{BVM} and T_{BHM} represent the values computed form the SMAP or Aquarius GMF [6,7]. The subscript "i" represents the data from two looks (fore and aft). The weighting coefficients, ΔT_{BV} and ΔT_{BH}, correspond to the noise-equivalent-delta-temperature (NEDT) of radiometer observations.

For this wind speed and direction (WD) retrieval algorithm during hurricane conditions, we provide the ancillary SSS from HYCOM [8] as input to the geophysical model function because T_Bs of vertical and horizontal polarizations essentially have the same sensitivity to wind speed above 20 m/s and consequently do not allow simultaneous wind speed, wind direction, and salinity retrieval. In general, there are multiple local minima (ambiguities) in the 2-dimensional speed and direction space. To improve the consistency of directional retrieval in the swath, we apply median filtering technique for ambiguity removal [9] and the Directional Interval Retrieval with THreshold (DIRTH) nudging technique developed for QuikSCAT wind processing [10].

@Copyrights reserved, 2016

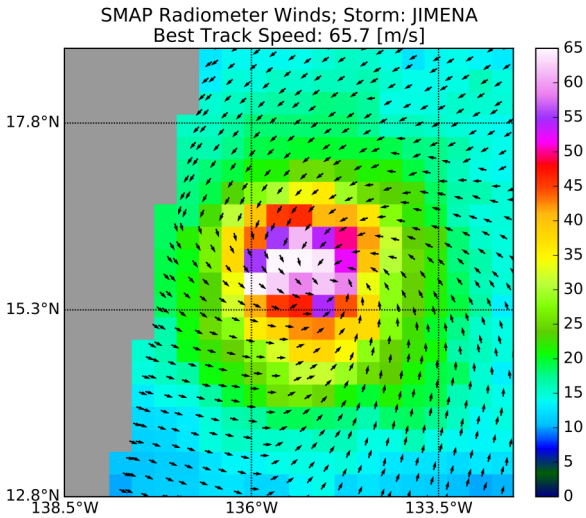

Figure 1. SMAP radiometer wind image of hurricane Jimena. The SMAP maximum wind speed was about 65 m/s, in excellent agreement with the NHC best track analysis.

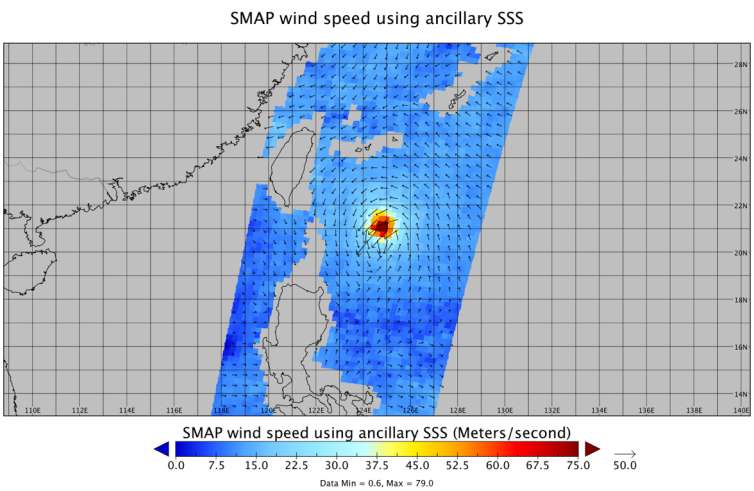

Figure 2. SMAP ocean vector wind of Typhoon Nepartak at near 22 UT on July 6, 2016.

We have also applied a wind speed and sea surface salinity (WS) retrieval algorithm [5] to the SMAP T_B data. This algorithm includes one additional term in the cost function with a constraint on the wind speed solution using the National Center for Environmental Predictions (NCEP) wind speed (w_{NCEP}) [11]:

$$C(w,SSS)=\sum_{i=1}^{2}\frac{(T_{BVi}-T_{BVMi})^2}{\Delta T_{BV}^2}+\sum_{i=1}^{2}\frac{(T_{BHi}-T_{BHMi})^2}{\Delta T_{BH}^2}+\frac{(w-w_{NCEP})^2}{\Delta w^2} \tag{2}$$

The weighting (Δw) on the wind speed difference is set at 1.5 m/s to primarily constrain the solution for high winds. The choice of 1.5 m/s for Δw can be justified through after the fact analysis of wind speed accuracy of about 1.1 m/s for retrieved wind under 20 m/s. The NCEP wind direction is also used as ancillary for the evaluation of geophysical model function. This wind speed and SSS retrieval algorithm is not applicable to very high wind speeds, and its output will be used for relative assessment of the hurricane wind retrieval algorithm described by Eq. (2) for wind speeds up to 20 m/s.

@Copyrights reserved, 2016

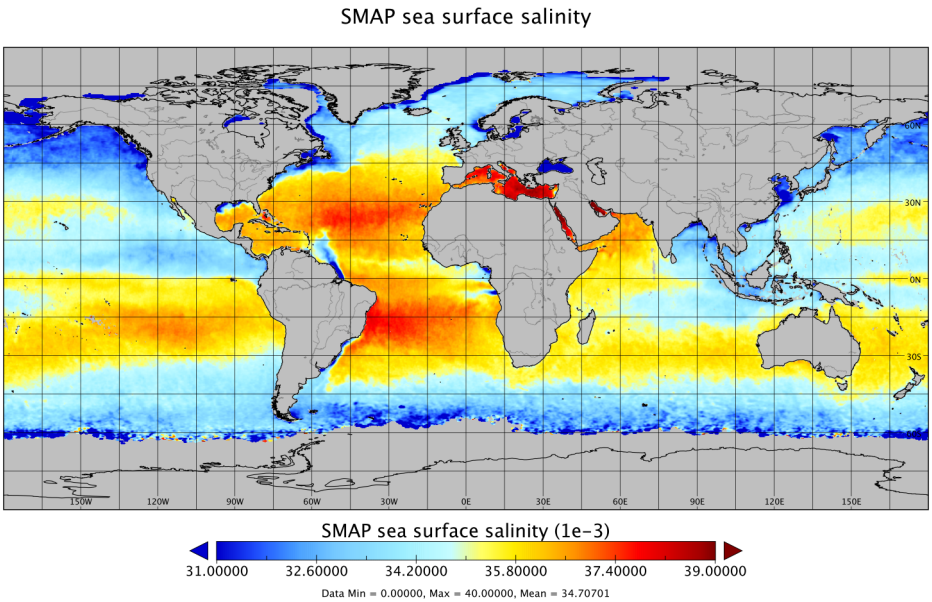

Figure 3. SMAP sea surface salinity averaged over one year of data acquired since April 2015.

Figure 1 illustrates one of the SMAP wind images of Hurricane Jimena in late August-early September 2015. Jimena was a category-4 hurricane with its maximum wind speed reaching 140 knots (or about 70 m/s) in late August. The SMAP wind direction appears reasonable, indicating closed circulation of winds around the eye. The National Hurricane Center (NHC) best track data showed that Jimena grew significantly in intensity from August 27 to 30, and the hurricane was near its peak strength on August 31 and September 1. The wind image for Jimena also reveals that the wind patterns are asymmetric around the eye with the regions of maximum wind generally located to the right hand side of the track; this asymmetric feature is primarily due to the forward motion of hurricane added to the inflow of surface winds toward the eye. Overall the features of SMAP radiometer wind vectors of Jimena appear reasonable.

Figure 2 provides one more example of the SMAP wind for a category 4 storm, illustrating the vector wind of Typhoon Nepartak. Its exceptionally strong wind and excessive rainfall caused significant damage in Taiwan during its landfall. The maximum wind speed in the SMAP wind image is 79 m/s, in excellent agreement with the best track wind speed of 77 m/s provided by the Joint Typhoon Warning Center (JTWC).

The sea surface salinity retrieved from SMAP data is illustrated in Fig. 3. The spatial pattern agrees with the climatological distributions of precipitation and evaporation in the Pacific and Atlantic. The salinity in the mid-Atlantic, primarily reflecting more evaporation than precipitation, is in the range of 35 to 37 practical salinity unit (psu). The high salinity in the Mediterranean, Red Sea and Persian Gulf is also evident. The Pacific is fresher with a lower salinity (32-35 psu) than the Atlantic due to excess rainfall, in particular in the Inter-Tropical Convergence Zone (ITCZ), North and Western Pacific. The image also reveals the fresh water plumes from the Amazon, Mississippi, Congo, and Gange Rivers. The freshwater plume associated with the Amazon can move to the north and east through advection by more than a thousand km over months.

@Copyrights reserved, 2016

VALIDATION

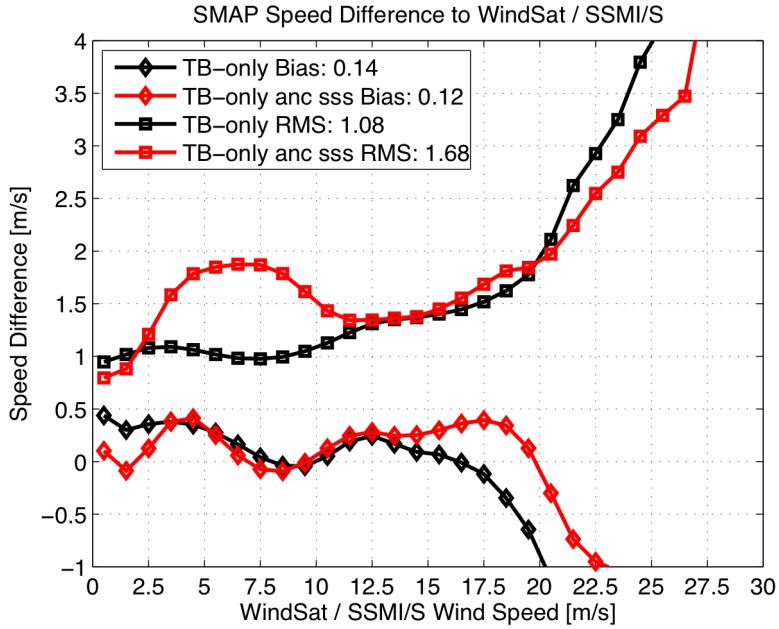

Figure 4. Comparison of the SMAP radiometer wind speed with the WindSAT and SSMIS wind speeds. The data for two SMAP radiometer products are illustrated: Black for the wind speed and salinity algorithm and red for the wind speed and direction algorithm, which uses the HYCOM salinity for ancillary.

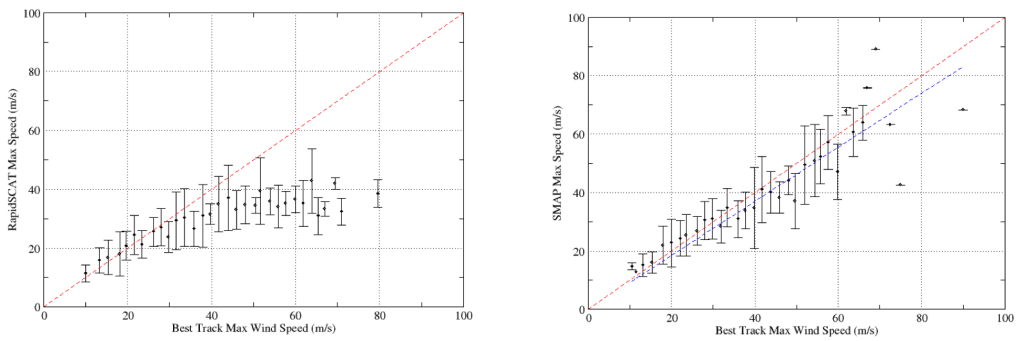

Figure 5. Comparison of SMAP and RapidSCAT maximum wind speeds with the best track analysis. Left: Rapdiscat; Right: SMAP.

We assess the SMAP radiometer winds in two wind speed regimes, 1) one for wind speeds lower than 20 m/s and 2) the other for higher wind speeds, by comparison with the wind products from other satellites and numerical weather models. For the lower wind speed regime, we carry out a comparative analysis with the wind speeds from WindSat or SSMIS [12] and the wind direction from the European Center for Medium Range Weather Forecasts (ECMWF). For the high wind regime, we apply the best track analysis for comparison of wind structure maxima.

We collocate the SMAP radiometer wind with the ECMWF wind by temporally interpolating the ECMWF winds before and after the SMAP pass. For the WindSat and SSMIS collocation, the data acquired within 15 minutes is used. The bias and standard deviation of the two SMAP radiometer wind speed products, including the one derived from the WS algorithm and the one retrieved from the WD algorithm (using the ancillary HYCOM SSS), computed with respect to the

@Copyrights reserved, 2016

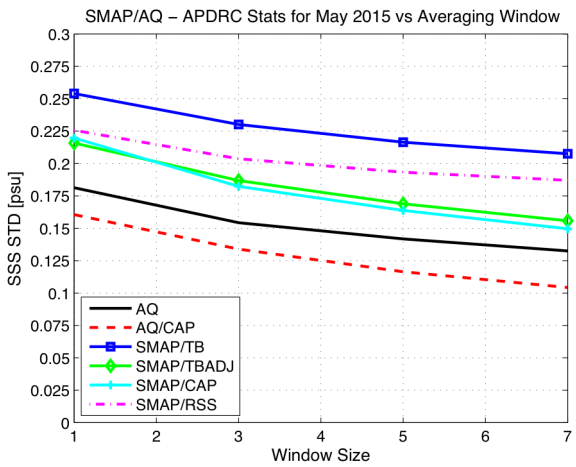

Figure 6. Comparison of SMAP and Aquarius SSS products with the ARGO gridded product for the month of May 2015. AQ: SSS from Aquarius Data Processing System (ADPS); AQ/CAP: Aquarius SSS produced by Jet Propulsion Laboratory (JPL) using Combined Active and Passive (CAP) algorithm; SMAP/TB: SMAP SSS derived from brightness temperature by JPL; SMAP/TBADJ: JPL SMAP SSS with latitudinal bias removed; SMAP/CAP: JPL SMAP SSS derived using both radar and radiometer data; SMAP/RSS: SMAP SSS produced by the Remote Sensing Systems (beta version).

WindSat or SSMIS wind speed are compared in Fig. 4. The bias for the WD algorithm product (red) is under 0.5 m/s over the wind speed range of 0 to 20 m/s, and the RMSD is about 1.68 m/s. We have included the error analysis of the WS algorithm product derived from the SMAP radiometer data with the cost function specified by Eq. (3) [5]. This alternate wind algorithm uses the SMAP dual-polarized TB data to retrieve the wind speed and salinity, and uses the NCEP wind as ancillary. We perform a similar matchup for this alternate wind speed product, labeled by TB-only in Fig. 4, with the ECMWF/WindSAT/SSMIS wind. The bias of the WS wind speed is also small, but the RMSD is 1.08 m/s. The primary difference between this WS wind product and the SMAP radiometer vector wind product is the introduction of the ancillary HYCOM salinity in the WD algorithm for vector retrieval. The HYCOM SSS is known to have a saltier bias in parts of Eastern Pacific and Western Atlantic where precipitation and freshwater plume from river discharge are significant for the surface salinity. In any case, the accuracy of the wind speed for the WD vector wind is reasonable for wind speeds below 20 m/s.

The assessment of SMAP radiometer wind speed above hurricane force (>33m/s) has been performed by comparison with the maximum wind speed in the best track (BT) analysis for all storms that have reached above category 1 during their lifetime. There are 22 storms with the NHC BT analyses, and 32 storms with the Joint Typhoon Warning Center (JTWC) BT analyses through the end of March 2016. We have obtained a total of 105 SMAP passes for comparison with the NHC BT, and 172 passes with the JTWC BT. These storms include many category 4 and 5 cyclones in the Pacific, such as Jimena, Nangka, Dolphin, Noul, Chan_Hom, and Ignacio. We find the maximum wind speed in the retrieved SMAP data within about 80 km from the eye. The location of the eye is interpolated from the BT analysis to the time of SMAP observations.

We have performed an uncertainty analysis by grouping the SMAP maximum wind speeds in BT wind speed bins at 2 m/s intervals. For each wind speed bin, we compute the mean of the grouped SMAP maximum wind speeds ($\overline{W}_{SMAP}$) and the mean of BT wind speed ($\overline{W}_{BT}$). We have also computed the standard deviation of the grouped data in each bin. The mean and standard deviation are illustrated in Fig. 5 for retrievals using the SMAP GMF. The average of standard deviations for the maximum wind speed bins greater than 20 m/s is 7.4 m/s for retrieval using the SMAP GMF. This is a very similar value compared to what was found from SMOS data at similar spatial resolution [4]. The regression of the mean with the BT wind is

$$\overline{W}_{SMAP} = 0.92\overline{W}_{BT} \tag{3}$$

Here W_{SMAP} is the maximum wind speed from SMAP, and W_{BT} represents the 1-minute sustained maximum wind speed from the best track from JTWC or NHC.

@Copyrights reserved, 2016

In comparison, similar correlative analysis between the maximum wind speeds from RapidSCAT and Best Track indicates that the Ku-band scatterometer data from RapidSCAT can reach saturation above 40 m/s wind speed (Fig. 5), likely due to the significant attenuation of Ku-band signals by heavy precipitation near tropical cyclones. Cross-comparison of the SMAP and RapidScat results in Fig. 5 indicates the advantage of ocean wind products derived from L-band radiometer data.

For the validation of SMAP SSS, we have computed the bias and standard deviation of the differences with the ARGO monthly gridded product produced by the Asia-Pacific Data-Research Center (APDRC) at a range of spatial scales. We gridded the SMAP data at 100 km spatial resolution, which correspond to the window size of 1 (Fig. 6). The standard deviations of several products are illustrated in Fig. 6 for the data acquired between 40°N and 40°S latitudes. As shown, the Aquarius Combined Active Passive (CAP) SSS [12,13] has the smallest standard deviation, about 0.16 psu, whereas the SMAP SSS products have a standard deviation of about 0.22 for the SMAP/CAP algorithm and 0.25 psu (SMAP TB-only algorithm). We also increase the window size to up to 7, which correspond to the spatial average of 700 km, to understand the impact of spatial scale on accuracy assessment. Increasing the window size (or degrading the spatial resolution of SMAP and Aquarius SSS) reduces the standard deviation between satellite salinities and APDRC ARGO. The reduction is likely due to the coarser resolution in the APDRC ARGO gridded product than the SMAP product. The changes indicate the higher spatial resolution content in the SAMP and Aquarius SSS products.

SUMMARY

NASA's Soil Moisture Active Passive (SMAP) mission was launched to provide high-resolution, frequent-revisit global mapping of soil moisture. SMAP has two instruments, a polarimetric radiometer and a multi-polarization radar. Both instruments operate at L-band frequencies (~ 1GHz) and share a single 6-m rotating mesh antenna, producing a fixed incidence angle conical scan at 40° across a 1000-km swath and a 2-3 day global revisit. The radiometer has been operating since April 2015 with no issues. The radar also started operation in April, but ceased operation on July 7. We have performed the matchup of the SMAP data with the ocean surface wind and air temperature from the National Center for Environment Predictions, Special Sensor Microwave/Imager, HYCOM's sea surface salinity, and Reynolds sea surface temperature. We find that the SMAP data are in excellent agreement with the geophysical model function derived from the Aquarius data up to a wind speed of 20 ms^{-1}.

We applied the L-band GMF to the retrieval of ocean surface wind and SSS from the SMAP data by leveraging the QuikSCAT algorithms to account for the two-look geometry (fore and aft looks from the conical scan) and dual-polarization observations. The retrieval algorithm has been applied to about all available SMAP radiometer and radar data. Comparison with the European Center for Medium-Range Weather Forecasting, WindSat and RapidSCAT wind speeds suggests that SMAP's radiometer wind speed reaches an excellent accuracy of about 1.1-1.7 ms^{-1} below a wind speed of 20 ms^{-1}. We have also found that the maximum wind speed derived from the SMAP radiometer data can reach 140 knots for severe storms and are generally in good agreement with the hurricane track analysis for typhoons Nangka, Dolphin, and Noul. We have performed error analysis of SMAP's SSS products. The spatial patterns of the SMAP SSS agree well with climatological distributions, but exhibit several unique spatial and temporal features. The temporal evolutions of freshwater plumes from several major rivers, such as the Amazon, Niger, Congo, Ganges, Salween, and Mississippi, are all consistent with the timing of rainy and dry seasons, indicated in the SMAP's soil moisture products. Our results indicate that the SMAP L-band microwave data will be useful for ocean weather monitoring and research.

ACKNOWLEDGEMENT

The work described in this paper was carried out by the Jet Propulsion Laboratory, California Institute of Technology under a contract with the National Aeronautics and Space Administration. N. Reul would like to acknowledge the support of the ESA Support to Science Element program under the contract SMOS + STORM evolution, #4000105171/12/I-BG.

@Copyrights reserved, 2016

REFERENCES

[1] Entekhabi, D., Njoku, E. G., O'Neill, P. E., Kellogg, K. H., Crow, W. T., Edelstein, W. N., Entin, J. K., Goodman, S. D., Jackson, T. J., Johnson, J., Kimball, J., Piepmeier, J. R., Koster, R. D., Martin, N., McDonald, K. C., Moghaddam, M., Moran, S., Reichle, R., Shi, J. C., Spencer, M. W., Thurman, S. W., Tsang, L., and J. Van Zyl, "The Soil Moisture Active Passive (SMAP) Mission," Proceedings of IEEE, Vol. 98,No. 5,pp. 704-716 (2010).

[2] Font, J., Camps, A., Borges, A., Martin-Neira, M., Boutin, J., Reul, N., Kerr, Y. H., Hahne, A., and Mecklenburg, S.. "SMOS: The Challenging Sea Surface Salinity Measurement from Space," Proceedings of the IEEE, Vol. 98, No. 5, doi: 10.1109/jproc.2009.2033.

[3] Reul, N., Tenerelli, J., Chapron, B., Vandemark, D., Quilfen, Y., and Kerr, Y , "SMOS satellite L-band radiometer: A new capability for ocean surface remote sensing in hurricanes, " J. Geophysical Research-Oceans, Volume: 117, FEB 2 2012.

[4] Reul, N., Chapron, B., Zabolotskikh, E., Donlon, C., Quilfen, Y., Guimbard, S., Piolle, J. F., "A revised L-band radio-brightness sensitivity to extreme winds under tropical cyclones: The 5 year SMOS-Storm database," Remote Sensing of Environemnt, 180, 274-291 (2016).

[5] Fore, A. G., Yueh, S. H., Tang, W., Stiles, B. W., and Hayashi, A. K., "Combined Active / Passive Retrievals of Ocean Vector Wind and Sea Surface Salinity with SMAP," IEEE Trans. Geoscience and Remote Sens., in press, 2016.

[6] Yueh, S. H., Tang, W., Fore, A., Hayashi, A., Song, Y. T., and Lagerloef, G., "Aquarius geophysical model function and combined active passive algorithm for ocean surface salinity and wind retrieval", *J. Geophys. Res. Oceans,* 119, 5360–5379 (2014).

[7] Yueh, S. H., Tang, W., Fore, A., Neumann, G., Hayashi, A., Freedman, A., Chaubell, J., and Lagerloef, G., "L-band Passive and Active Microwave Geophysical Model Functions of Ocean Surface Winds and Applications to Aquarius Retrieval." *IEEE Trans. Geoscience and Remtoe Sensing*, 51 (9), 4619-4632 (2013).

[8] Chassignet, E.P., Hurlburt, H.E., Metzger, E.J., Smedstad, O.M., Cummings, J., Halliwell, G. R., Bleck, R., Baraille, R., Wallcraft, A. J., Lozano, C., Tolman, H. L., Srinivasan, A., Hankin, S., Cornillon, P., Weisberg, R. Barth, A., He, R., Werner, F., and Wilkin, J., "U.S. GODAE: Global Ocean Prediction with the HYbrid Coordinate Ocean Model (HYCOM)." Oceanography, 22(2), 64-75 (2009).

[9] Shaffer, S. J., Dunbar, R. S., Hsiao, S. V., and Long, D. G., "A Median-Filter-Based Ambiguity Removal Algorithm For NSCAT," IEEE Trans. Geosci. Remote Sens., Vol. 29. No. 1. Pp. 167-174 (1991).

[10] Stiles, B., Pollard, B., and Dunbar, R., "Direction interval retrieval with thresholded nudging: a method for improving the accuracy of QuikSCAT winds," IEEE Transactions on Geoscience and Remote Sensing, vol. 40, no. 1, pp. 79–89 (2002).

[11] NCEP Global Forecast System products, http://nomads.ncdc.noaa.gov/data.php#hires_weather_datasets

[12] WindSAT and SSMI/S products produced by the Remote Sensing System, http://www.ssmi.com/

@Copyrights reserved, 2016